EURASIP Journal on Advances in Signal Processing
a SpringerOpen Journal

RESEARCH Open Access

A novel ULA-based geometry for improving AOA estimation

Shahriar Shirvani-Moghaddam[1*] and Farida Akbari[2]

Abstract

Due to relatively simple implementation, Uniform Linear Array (ULA) is a popular geometry for array signal processing. Despite this advantage, it does not have a uniform performance in all directions and Angle of Arrival (AOA) estimation performance degrades considerably in the angles close to endfire. In this article, a new configuration is proposed which can solve this problem. Proposed Array (PA) configuration adds two elements to the ULA in top and bottom of the array axis. By extending signal model of the ULA to the new proposed ULA-based array, AOA estimation performance has been compared in terms of angular accuracy and resolution threshold through two well-known AOA estimation algorithms, MUSIC and MVDR. In both algorithms, Root Mean Square Error (RMSE) of the detected angles descends as the input Signal to Noise Ratio (SNR) increases. Simulation results show that the proposed array geometry introduces uniform accurate performance and higher resolution in middle angles as well as border ones. The PA also presents less RMSE than the ULA in endfire directions. Therefore, the proposed array offers better performance for the border angles with almost the same array size and simplicity in both MUSIC and MVDR algorithms with respect to the conventional ULA. In addition, AOA estimation performance of the PA geometry is compared with two well-known 2D-array geometries: L-shape and V-shape, and acceptable results are obtained with equivalent or lower complexity.

Keywords: array processing, antenna array geometry, ULA, L-shape, V-shape, AOA, DOA, MUSIC, MVDR

Introduction

Signal processing using an array of sensors provide more capability than a single sensor through analysis of wavefields [1]. An array of sensors is exploited to collect signals impinging on the array sensors which may be antennas, microphones, hydrophones and etc. These signals, which have little difference in amplitude and phase, are processed and signal parameters such as Direction of Arrival (DOA), Time of Arrival (TOA), Time Difference of Arrival (TDOA), polarization, frequency, and number of signal sources or a joint of these cases [2,3] can be estimated. Therefore, array signal processing can be utilized in various fields such as radar, sonar, navigation, geophysics, acoustics, astronomy, medical diagnosis and wireless communications.

DOA or Angle of Arrival (AOA) is an important signal parameter which may be used for source localization or source tracking by determining the desired signal location or may be exploited to reduce the unwanted effects of noise and interference. AOA estimation plays a key role in enhancing the performance of adaptive antenna arrays for mobile wireless communications. It can improve the system performance by helping the channel modeling and suppression of undesirable signals like multipath fading and Co-Channel Interference (CCI). In adaptive array antennas or smart antenna systems, AOA estimation algorithms provide information about the system environment for an efficient beamforming or for providing location-based services such as emergency services [4-9]. Therefore, great lines of research have been accomplished about AOA estimation during last recent decades. Various AOA estimation methods have been proposed in the literature. These methods differ in technique, speed, computational complexity, accuracy and their dependency on the array structure and signal as well as channel characteristics. Different methods have been suggested to enhance the performance of available algorithms including increasing the accuracy and resolution of AOA estimation algorithms.

* Correspondence: sh_shirvani@srttu.edu
[1]Digital Communications Signal Processing (DCSP) Research Lab., Faculty of Electrical and Computer Engineering, Shahid Rajaee Teacher Training University (SRTTU), Tehran, Iran
Full list of author information is available at the end of the article

Most of efforts tried to use statistical approaches to achieve more accuracy. This manner may lead to extra complexity and additional computations.

Beside the algorithms, location of the elements in an array strongly affects the AOA estimation performance. A considerable amount of work has been done on design of arrays to achieve or optimize the array performance that include terms such as cost, space, variance of error or resolution limits [10]. The investigation of antenna arrays is often based on Uniform Linear Array (ULA) geometry because of simple analysis and implementation. However, this topology has some drawbacks. For example, the ULA is 1-D and so it is capable for AOA estimation in one-dimensional applications, however, today's applications interest in multi-dimensional (M-D) AOA estimation. Thus, planar arrays and 3-D arrays are needed to be exploited. Another drawback of the ULA is that it does not have uniform performance; the AOA estimation performance degrades considerably close to endfire directions. This major drawback can be resolved by employing other array geometries.

Some array configurations have been suggested to improve the performance of AOA estimation and beamforming process in the literature. Uniform Circular Array (UCA) is a most nonlinear investigated configuration [11,12]. A combination of linear arrays can be used for M-D AOA estimation or improving the performance of the ULA. Some topologies such as, one L-shape and two L-shape arrays for AOA estimation in planar and volume mode have been examined [13-15]. Y-shaped distribution of elements is also used to achieve uniform AOA detection performance [16]. The array with a V-shape structure, which is suitable for 120 degrees sectored cellular systems, is proposed for 2-D [17] and 3-D DOA estimation [18]. In addition, ref. [19] shows DOA estimation improvement in uniform and non-uniform arrangements.

In ref. [20], different types of array structures for smart antennas (ULA, UCA and Uniform Rectangular Array (URA)), AOA estimation and beamforming performance have been examined. Another research has concentrated on arrays that have uniform performance over the whole field of view and isotropic AOA estimation [10]. Some other known geometries such as, different circular arrangements and hexagonal configuration have been also examined for smart antenna applications [21], but many of these geometries may lead to further complexity of array structure and calculations, and array aperture may become larger. Thus, it is desirable to develop simple array configurations which perform uniform in all directions. In this regard, Displaced Sensor Array (DSA) is such a configuration which has presented equally improved performance for all azimuth angles [22].

In this article, it is attempted to present another simple ULA-based arrangement which improves the AOA estimation performance in comparison with the simple ULA configuration. Proposed Array (PA) adds two elements to the ULA in top and bottom of the array axis. This article focuses on smart antenna applications, but the utilization can be extended to other fields of sensor array processing. The accuracy and resolution threshold of two well-known AOA estimation algorithms, MUltiple SIgnal Classification (MUSIC) and Minimum Variance Distortionless Response (MVDR), are compared to evaluate the performance of the simple ULA, PA, L-shape and V-shape arrays. Simulation results show higher resolution of both algorithms in new proposed array with respect to the conventional ULA. The PA also performs better than the L-shape array in boresight directions. It also presents near results to the V-shape array with lower complexity and computational cost. This arrangement only adds two elements to the linear array in the vertical direction. Therefore, complexity and size of the proposed array does not increase too much.

The rest of article is organized as follows. 'Smart antennas' section describes smart antenna systems, briefly. Signal model for the ULA and the proposed array are stated in 'Signal model for the ULA and PA configurations' section. Consequently, 'AOA estimation methods' section provides a brief overview of AOA estimation methods and describes the MUSIC and MVDR algorithms. In 'Simulation results' section, simulation results using the MATLAB are presented. These results include the effect of number of data snapshots, effect of different SNRs considering boresight and endfire directions and comparison of the array configurations (ULA, PA, L-shape and V-shape arrays) in AOA estimation performance, estimation accuracy as well as resolution, and also their computational complexity. Finally, conclusion remarks are given in 'Conclusions' section.

Smart antennas

The fast growth of wireless communication networks has made an increasing demand for spectrum and radio resources. Smart antennas or adaptive array antennas are effective techniques for improvement of wireless systems performance. A smart antenna system merges an antenna array and a signal processing unit to combine the received signals in an adaptive manner and reach to the optimum performance for the system.

Beamforming algorithms are used to adjust the complex weights and to generate main lobes and nulls in the direction of desired and undesired signals, respectively. Furthermore, many users can be served in parallel by exploiting multi-beam radiation pattern and so, increased spectral efficiency can be obtained [4-7]. The received signals to the array are weighted and then combined together to form the radiation pattern of the array antenna. In addition, array weights are adjusted using

adaptive beamforming algorithms in order to optimize the performance of antenna system respect to the signal environment.

Signals are propagated from different sources and multipath fading provides different paths for them. For adaptive beamforming, the system needs to separate the desired signals from interferences. Therefore, either a reference signal or direction of signal sources will be required [7]. Various methods of beamforming and AOA estimation are available which differ in accuracy, computational complexity and convergence speed.

Antenna array consists of a set of antenna sensors, which are combined together in a particular geometry which may be linear, circular, planar, and conformal arrays commonly [5]. ULA is the most common geometry for smart antennas because of its simplicity, excellent directivity and production of the narrowest main lobe in a given direction in comparison to the other array geometries [22]. In a ULA, as it is seen in Figure 1, the elements are aligned along a straight line and with a uniform inter-element spacing usually $d = \lambda/2$, where λ denotes the wavelength of the received signal. If $d < \lambda/2$, mutual coupling effects cannot be ignored and the AOA estimation algorithm cannot generate desired peaks in the angular spectrum. On the other hand, if $d > \lambda/2$, then the spatial aliasing leads to misplaced or unwanted peaks in the spectrum. As so, $d = \lambda/2$ is the optimum inter-element spacing in the ULA configuration.

However, as mentioned before, the ULA does not work equally well for all azimuth directions and the AOA estimation accuracy and resolution are low at array endfires. In this section, a simple ULA-based is proposed to improve AOA estimation accuracy at endfire angles. This configuration is illustrated in Figure 2.

Signal model for the ULA and PA configurations

Received signals can be expressed as linear combination of incident signals and zero mean Gaussian noise. The incident signals are assumed to be direct line of sight and uncorrelated with the noise. The input signal vector denoted by $\boldsymbol{x}(t)$ can be written as:

$$\boldsymbol{x}(t) = \sum_{m=1}^{M} \boldsymbol{a}(\theta_m) s_m(t) + n(t) = \boldsymbol{A} \cdot \boldsymbol{S} + n \tag{1}$$

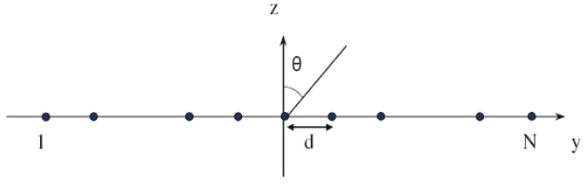

Figure 1 Uniform linear array (ULA) geometry.

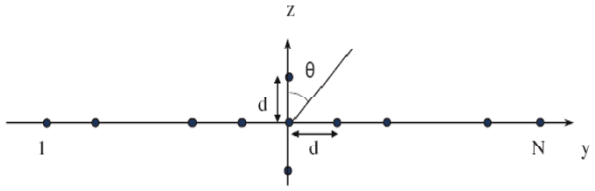

Figure 2 Proposed array (PA) geometry.

where M shows the number of incident signals on the array. $s_m(t)$ is the waveform for the m-th signal source at direction θ_m from the array boresight and $\boldsymbol{S}$ denotes the $M \times 1$ vector of the received signals. $\boldsymbol{a}(\theta_m)$ is the $N \times 1$ steering vector or response vector of the array for direction of θ_m, where N is the element number. Furthermore, $\boldsymbol{A}$ is a $N \times M$ matrix of steering vectors, which is named manifold matrix.

$$\boldsymbol{A} = \left[a(\theta_1) \quad a(\theta_2) \quad \ldots \quad a(\theta_M)\right] \tag{2}$$

The spatial correlation matrix of the received signals, $\boldsymbol{R}_{xx}$, is defined by:

$$\boldsymbol{R}_{xx} = E[x(t) \cdot x^H(t)] \tag{3}$$

where $E[.]$ is the expectation operator and H is the conjugate transposition operator. Substituting (1) into (3), $\boldsymbol{R}_{xx}$ can be written as:

$$\boldsymbol{R}_{xx} = E[\boldsymbol{A} \cdot \boldsymbol{s}(t) \cdot \boldsymbol{s}^H(t) \cdot \boldsymbol{A}^H] + E[\boldsymbol{n}(t) \cdot \boldsymbol{n}^H(t)] \tag{4}$$

And finally the spatial correlation matrix can be expressed as:

$$\boldsymbol{R}_{xx} = \boldsymbol{A}\boldsymbol{R}_{ss}\boldsymbol{A}^H + \sigma_n{}^2\boldsymbol{I} \tag{5}$$

$\boldsymbol{R}_{ss}$ shows the $M \times M$ signal correlation matrix. $\sigma_n{}^2$ and $\boldsymbol{I}$ are variance of noise and identity matrix, respectively. Since the antennas cannot receive DC signals, the mean values of arriving signals and noise are zero and so, the correlation matrix obtained in (5) is referred as covariance matrix [22]. This matrix is used for many beamforming and AOA estimation algorithms such as MUSIC and MVDR.

The array configuration, affects steering vectors and dimension of signal vector. In order to investigate the proposed array performance in AOA estimation of narrowband signals, a ULA with N elements and PA with $N + 2$ elements, as depicted in Figures 1 and 2, are compared. Both of the arrays are assumed symmetric around the origin. Therefore, N is assumed to be an odd number. The manifold matrix of the ULA and PA have dimensions of $N \times M$ and $(N + 2) \times M$, respectively.

If $\boldsymbol{a}_{\mathrm{ULA}}(\theta_m)$ represents the steering vector for each of the input signals on the linear array, then for the

symmetrical linear array, $\boldsymbol{a}_{\mathrm{ULA}}(\theta_m)$ can be written as a $N \times 1$ vector expressed as:

$$\boldsymbol{a}_{ULA}(\theta_m) = \begin{bmatrix} e^{-j}\left(\frac{N-1}{2}\right)k.d\sin\theta_m \\ e^{-j}\left(\frac{N-2}{2}\right)k.d\sin\theta_m \\ \vdots \\ e^{j}\left(\frac{N-2}{2}\right)k.d\sin\theta_m \\ e^{j}\left(\frac{N-1}{2}\right)k.d\sin\theta_m \end{bmatrix} \quad (6)$$

where d is the inter-element space and $k = 2\pi/\lambda$.

Steering vector for the proposed array is represented with $\boldsymbol{a}_{\mathrm{PA}}(\theta_m)$ that is a $(N + 2) \times 1$ vector and it can be written as:

$$\boldsymbol{a}_{PA}(\theta_m) = \begin{bmatrix} e^{-j}\left(\frac{N-1}{2}\right)k.d\sin\theta_m \\ e^{-j}\left(\frac{N-2}{2}\right)k.d\sin\theta_m \\ \vdots \\ e^{j}\left(\frac{N-2}{2}\right)k.d\sin\theta_m \\ e^{j}\left(\frac{N-1}{2}\right)k.d\sin\theta_m \\ e^{jk.d\cos\theta_m} \\ e^{-jk.d\cos\theta_m} \end{bmatrix} \quad (7)$$

The first N rows of $\boldsymbol{a}_{PA}(\theta_m)$ are related to the linear part of the array and two remained rows show the effect of the top and bottom elements in the proposed array.

AOA estimation methods

AOA estimation algorithms are classified into four categories; Conventional, Subspace-based, Maximum Likelihood-based and Subspace fitting techniques. The two first methods are spectral-based methods that rely on calculating the spatial spectrum of the received signals and finding the AOAs as the location of peaks in the spectrum. The third and fourth approaches are called parametric array processing methods that directly estimate AOAs without first calculating the spectrum. The parametric algorithms have higher performance in terms of accuracy and resolution. The cost for this performance improvement is higher complexity and more computations.

In each class of the above-mentioned four categories of AOA estimation approaches, various algorithms have been presented which differ in modeling approach, computational complexity, resolution threshold and accuracy [7,8]. The conventional techniques are based on beamforming where the array weights are adjusted and the spectrum presents maximum amounts at angles that the output power is maximized. Therefore, by searching the spectrum for location of peaks, signal sources are detected. The MVDR is a well-known conventional algorithm. These methods are easy to apply and need fewer calculations than the other methods, but they cannot provide a high resolution and accuracy. On the other hand, subspace-based techniques produce the spatial spectrum by using Eigen-decomposition of the covariance matrix of input signals, from which AOA is estimated. The MUSIC is a very common subspace-based algorithm [8].

In this article, two spectral-based algorithms, MVDR and MUSIC, are investigated. Related on the array structure and algorithm capability, AOA can be estimated in one or more dimensions. In order to compare the array accuracy in different directions for AOA estimation applications, AOA will be investigated in the plane $\phi = 0°$.

MUSIC algorithm

The Eigen-vectors of the covariance matrix belong to either of two orthogonal signal or noise subspaces. If M signals arrive on the array, the M Eigen-vectors associated with M larger Eigen-values of the covariance matrix span the signal subspace and the N - M Eigen-vectors corresponding to the N - M smaller Eigen-values of the covariance matrix span the noise subspace. The M steering vectors that form the manifold matrix $\boldsymbol{A}$ are orthogonal to the noise subspace and so the steering vectors lie in the signal subspace.

The MUSIC algorithm estimates the noise subspace using Eigen-decomposition of the sample covariance matrix and then the estimate of AOAs are taken as those θ that give the smallest value of $\boldsymbol{A}^{\mathrm{H}}(\theta)\cdot\boldsymbol{V}_n$, where $\boldsymbol{V}_n$ denotes the matrix of Eigen-vectors corresponding to the noise subspace. These values of θ result in a steering vector farthest away from the noise subspace and as orthogonal to the noise subspace as possible [4,7-9]. This is done by finding the M peaks in the MUSIC spectrum defined by:

$$P_{\mathrm{MUSIC}}(\theta) = \frac{1}{A^H V_n V_n{}^H A} \quad (8)$$

MVDR algorithm

In the MVDR approach, it is attempted to minimize the power contributed by noise and undesired interferences, while maintaining a fixed gain in the look direction, usually equal to unity. This is written as:

$$\min E[|\gamma(\theta)|^2] = \min \boldsymbol{w}^H \boldsymbol{R}_{xx}\boldsymbol{w}, \quad \boldsymbol{w}^H\boldsymbol{A}(\theta_0) = 1 \quad (9)$$

Using Lagrange multiplier technique, the weight vector that solves this equation is given by:

$$\boldsymbol{w} = \frac{\boldsymbol{R_{xx}}^{-1}\boldsymbol{A}}{\boldsymbol{A}^H\boldsymbol{R_{xx}}^{-1}\boldsymbol{A}} \tag{10}$$

The MVDR angular spectrum is defined by:

$$P_{\mathrm{MVDR}}(\theta) = \frac{1}{\boldsymbol{A}^H\boldsymbol{R_{xx}}^{-1}\boldsymbol{A}} \tag{11}$$

The peaks in the MVDR spectrum occur whenever the steering vector is orthogonal to the noise subspace, so the AOAs are estimated by detecting the peaks in the spectrum [7,23].

Simulation results

Comparison of the PA and conventional ULA

To compare the accuracy of the MUSIC and MVDR algorithms in both ULA and PA geometries, a ULA with $N = 15$ elements is assumed and therefore, the proposed array consists of $N = 17$ elements. Inter-element spacing is maintained $d = \lambda/2$. The signal to noise ratio is SNR = 10 dB and the interior signals are assumed uncorrelated. Also, the number of data snapshots is $K = 100$.

Both of arrays are simulated and compared in identical situations. Table 1 shows the effects of different number of data snapshots on AOA estimation accuracy. The MUSIC works appropriately with few snapshots. The MVDR needs more snapshots to work accurately, but this amount is not very high. It can be concluded that a proper accuracy can be achieved using lower number of data snapshots. Simulation results show that $K \geq 100$ leads to accurate and reliable results in AOA estimation through both the MUSIC and MVDR methods. Figures 3 and 4 depict RMSE diagrams in degree for AOA estimation of signal sources located at 10° and 85° with respect to SNR changes. As the SNR increases, RMSE of the estimated AOA decreases in both arrays. The PA has lower RMSE and therefore better accuracy than the ULA at endfire directions.

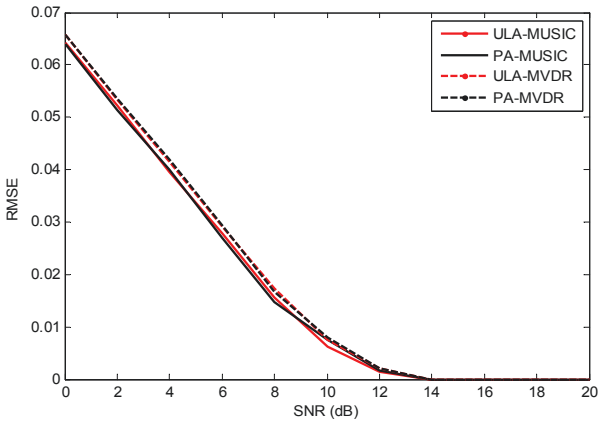

Figure 3 RMSE of the ULA and PA with respect to SNR variations at boresights (AOA = 10°), $K = 100$.

Figures 5 and 6 show the spatial spectrum in both ULA and PA at endfire angles (-85°, 85°) for the MUSIC and MVDR algorithms, respectively. Simulation results depict sharp peaks at the location of signal sources while the ULA spectrum shows ambiguity at the endfire directions that means AOAs have been missed. As a result, the drawback of the ULA at endfire directions is eliminated by using the new array geometry.

Figure 7 shows the MUSIC spectrum of both arrays to detect two close sources which are assumed around the array boresight at (-2°, 2°). The PA is capable to distinguish two close sources as well as the ULA and both arrays can generate separate peaks in the spatial spectrum for each of the assumed sources. Therefore, an identical accuracy and resolution can be achieved for the PA at boresight angles, where the ULA performs well.

The resolution threshold of the array is obtained with decreasing the angular difference between two close angles and investigating the array ability to form the correct peaks in the spectrum. In order to compare the arrays capability during AOA estimation algorithms, Monte Carlo approach is used to achieve more accurate

Table 1 Effect of the number of data snapshots on the accuracy of AOA estimation algorithms.

K (data snapshots)	AOA (°)	Estimated AOA by MUSIC		Estimated AOA by MVDR	
		θ (°)	Fluctuation in the spectrum	θ (°)	Fluctuation in the spectrum
10	10	10.2	Low	-	High
20	10	10	Low	10	Moderate
50	10	10	Negligible	10.1	Moderate
100	10	10	Negligible	10	Negligible
200	10	10	Negligible	10	Negligible
500	10	10	Negligible	10	Negligible
1000	10	10	Negligible	10	Negligible

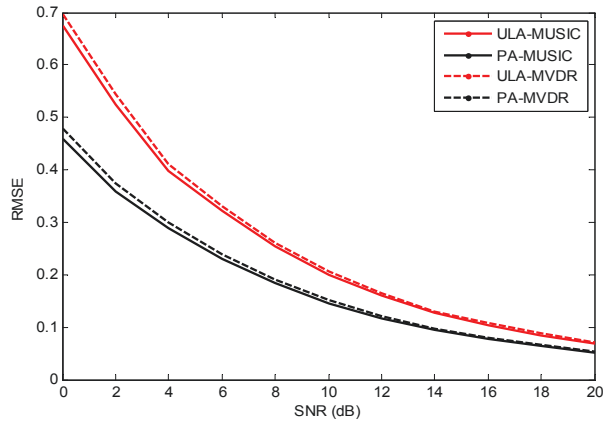

Figure 4 RMSE of the ULA and PA with respect to SNR variations at endfires (AOA = 85°), *K* = 100.

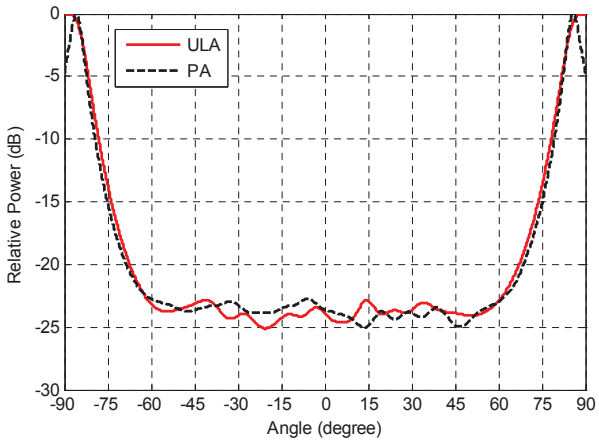

Figure 6 MVDR spectrum for the ULA and PA geometries at endfire AOAs (-85°, 85°), SNR = 10 dB, *K* = 100.

results. Each algorithm has been simulated 1000 times and final results have been calculated via averaging.

In Table 2, MUSIC resolution is investigated for two adjacent sources, assumed at middle of the spectrum. The sources are made so close together that the algorithm cannot distinguish them. This angle can be evaluated as the resolution threshold of the algorithm. Numerical results confirm similar accuracy and resolution of both arrays in detection of close sources at the middle of the spectrum.

A similar comparison is done for the MVDR. Figure 8 shows the capability of both array configurations in distinguishing close sources at middle of the spectrum. In Table 3, the resolution threshold of both arrays is compared via the MVDR algorithm. The peaks generated in the MVDR spectrum, aren't as sharp as the MUSIC spectrum, so the MVDR resolution is lower than the MUSIC.

Performance of the ULA and PA at endfire AOAs is seen in Figure 9 and Table 4, for resolving two closely sources. The PA presents higher accuracy and resolution than the ULA at endfires. It seems that both arrays have similar ability for resolving middle angles but as expected, the ULA has less accuracy than the proposed array for the angles located in both sides of the spectrum.

Figure 10 and Table 5 show similar results obtained via the MVDR algorithm at the endfire source locations. Spectral and numerical results confirm the higher accuracy and resolution of the proposed array configuration than the ULA, for AOAs located at border sides of the spectrum. Since lower resolution of the MVDR, the PA strength is better seen here.

In general, the complexity of the MUSIC and MVDR algorithms are of the order N^3, for Eigen-decomposition and inversion of input correlation matrix, respectively [24-26]. Therefore, adding two elements to the array

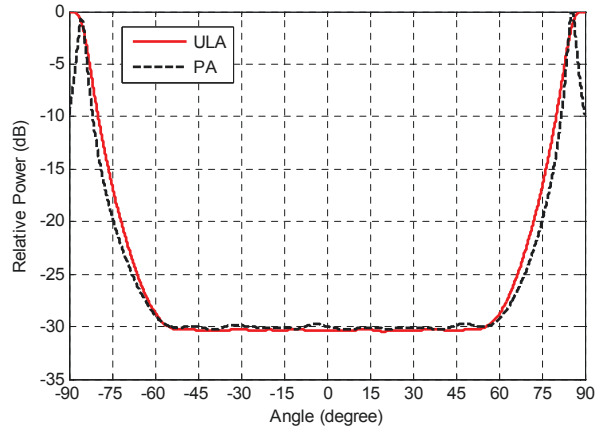

Figure 5 MUSIC spectrum for the ULA and PA geometries at endfire AOAs (-85°, 85°), SNR = 10 dB, *K* = 100.

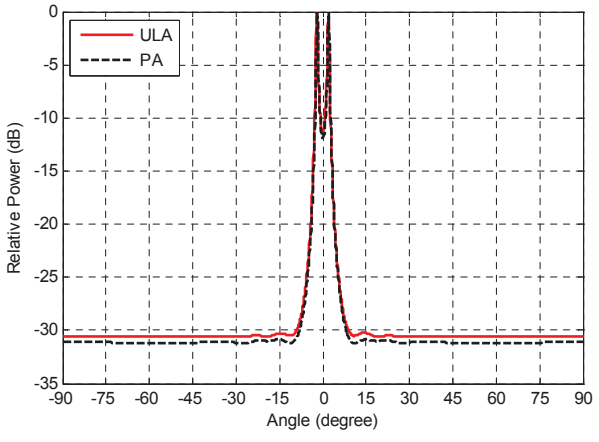

Figure 7 MUSIC spectrum for the ULA and PA geometries at boresight AOAs (-2°, 2°), SNR = 10 dB, *K* = 100.

Table 2 Accuracy of MUSIC algorithm in the case of narrowband sources at the middle of the spectrum, SNR = 10 dB, *K* = 100.

Angles (°)	Success (%)		Average of estimated angles (°)		Variance of estimated angles (°)	
	PA	ULA	PA	ULA	PA	ULA
θ1 = 30	100	100	30.0900	30.0873	0.0111	0.0133
θ2 = 33			32.9145	32.9160	0.0137	0.0131
θ1 = 30	100	100	30.1150	30.1085	0.0146	0.0156
θ2 = 32.8			32.6860	32.6856	0.0141	0.0176
θ1 = 30	99.5	98.9	30.1434	30.1471	0.0185	0.0213
θ2 = 32.6			32.4470	32.4510	0.0192	0.0226
θ1 = 30	80.9	80.5	30.1860	30.1772	0.0207	0.0263
θ2 = 32.4			32.1981	32.2026	0.0257	0.0312
θ1 = 30	24.4	24.8	30.1746	30.1592	0.0541	0.0565
θ2 = 32.2			32.0171	32.0348	0.0333	0.0368
θ1 = 30	1.7	1.9	30.5279	30.5583	0.1082	0.1284
θ2 = 32			31.6187	31.6420	0.0846	0.0765
θ1 = 30	0.1	0	30.6056	30.6207	0.0889	0.0891
θ2 = 31.8			31.2158	31.2160	0.1035	0.1162

causes that the computational load rise to order $(N + 2)^3$. The size of the ULA aperture affects the resolution threshold, especially at boresight directions. Hence if two elements at both ends of PA be lessened, computational cost remains the same, while the PA still performs well at endfire directions. Simulation results show that in this situation the resolution threshold may be a little decreased. Therefore, the increase in computational cost prevents the changes of resolution threshold in boresight directions.

Comparison of the PA and two other array geometries

Simulation results demonstrated better performance of the PA in detection and separation of signal sources located at array endfires with respect to the ULA. Similar comparison between the PA and other geometries can be investigated. In this work, two considerable arrangements, the L-shape and V-shape arrays, are applied for 1-D AOA estimation and their performance is compared with the PA. In the literature, planar L-shape array has shown good accuracy [13] and the V-shape structure with specified design has demonstrated isotropic and uniform performance in all directions [27].

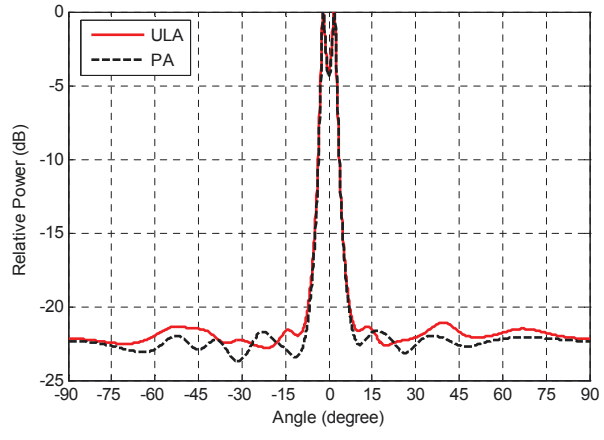

Figure 8 MVDR spectrum for the ULA and PA geometries at boresight AOAs (-2°, 2°), SNR = 10 dB, *K* = 100.

For simulation, three planar arrays, PA, L-shape and V-shape arrangements, with equal element numbers are assumed. The L-shape and V-shape structures are illustrated in Figures 11 and 12. Steering vector for these arrays can be written as (12), (13), respectively.

$$\boldsymbol{a}_{L-shape}(\theta_m) = \begin{bmatrix} e^{j\left(\frac{N-1}{2}\right)k.d\cos\theta_m} \\ e^{j\left(\frac{N-3}{2}\right)k.d\cos\theta_m} \\ \vdots \\ e^{jk.d\cos\theta_m} \\ 1 \\ e^{jk.d\sin\theta_m} \\ \vdots \\ e^{j\left(\frac{N-3}{2}\right)k.d\sin\theta_m} \\ e^{j\left(\frac{N-1}{2}\right)k.d\sin\theta_m} \end{bmatrix} \tag{12}$$

$$\boldsymbol{a}_{V-shape}(\theta_m) = \begin{bmatrix} e^{-j\left(\frac{N-1}{2}\right)\left(\frac{\sqrt{3}}{2}\right)k.d\sin\theta_m.e^{j\left(\frac{N-1}{2}\right)\left(\frac{1}{2}\right)k.d\cos\theta_m}} \\ e^{-j\left(\frac{N-3}{2}\right)\left(\frac{\sqrt{3}}{2}\right)k.d\sin\theta_m.e^{j\left(\frac{N-3}{2}\right)\left(\frac{1}{2}\right)k.d\cos\theta_m}} \\ \vdots \\ e^{j\left(\frac{N-3}{2}\right)\left(\frac{\sqrt{3}}{2}\right)k.d\sin\theta_m.e^{j\left(\frac{N-3}{2}\right)\left(\frac{1}{2}\right)k.d\cos\theta_m}} \\ e^{j\left(\frac{N-1}{2}\right)\left(\frac{\sqrt{3}}{2}\right)k.d\sin\theta_m.e^{j\left(\frac{N-1}{2}\right)\left(\frac{1}{2}\right)k.d\cos\theta_m}} \end{bmatrix} \tag{13}$$

Table 3 Accuracy of MVDR algorithm in the case of narrowband sources at the middle of the spectrum, SNR = 10 dB, *K* = 100.

Angles (°)	Success (%)		Average of estimated angles (°)		Variance of estimated angles (°)	
	PA	ULA	PA	ULA	PA	ULA
θ1 = 30	100	100	30.3378	30.3813	0.0150	0.0179
θ2 = 33.6			33.2452	33.2077	0.0159	0.0183
θ1 = 30	99.8	97.7	30.4297	30.5000	0.0237	0.0296
θ2 = 33.4			32.9558	32.8870	0.0240	0.0290
θ1 = 30	92.7	83.9	30.5642	30.6317	0.0416	0.0543
θ2 = 33.2			32.6238	32.5564	0.0338	0.0487
θ1 = 30	55	35	30.7901	30.9372	0.1381	0.1601
θ2 = 33			32.2243	32.0572	0.0918	0.1494
θ1 = 30	10.7	3	31.1459	31.2665	0.1678	0.1226
θ2 = 32.8			31.6801	31.5318	0.1645	0.1225
θ1 = 30	0.1	0	31.2599	-	0.0619	-
θ2 = 32.6			31.3259	-	0.0611	-

Steering vectors for the PA, L-shape and V-shape arrays are $N \times 1$ vectors. N that represents the number of elements is assumed 15 in this section. Angle of ULAs in the L-shape and V-shape arrays are assumed 90° and 120°, respectively. Figures 13 and 14 show the MUSIC and MVDR spectrums for detection and separation of signal sources placed at closed angles to the array endfires, respectively. The L-shape array presents sharper peaks at the source locations and higher ability in resolving close sources placed near to the endfires in comparison with other structures. The V-shape array and the PA also have detected and resolved the signal sources at endfires accurately.

In Figures 15 and 16, the MUSIC as well as the MVDR spectrums are shown for AOA estimation in the middle of the spectrum. Simulation results show that despite the high resolution of the L-shape array at border angles, this array does not present a well resolution in the middle of the spectrum. Therefore, the L-shape array does not have a uniform performance at all directions. Simulation results also show that the V-shape array and PA with equal element number, present almost similar results in the middle of the spectrum.

Computational complexity of AOA estimation algorithms includes two parts: steering vector calculations and matrix inversion in the MVDR or Eigen-decomposition in the MUSIC calculations. With equal element numbers, computational cost for AOA estimation algorithms is equivalent in the PA and L-shape arrays. However, steering vector for the V-shape array is obtained with more complexity and computational cost than the PA and L-shape arrays (compare Equations 7, 12 and 13). The PA also occupies less space than the V-shape array for utilization in base stations. In addition, the

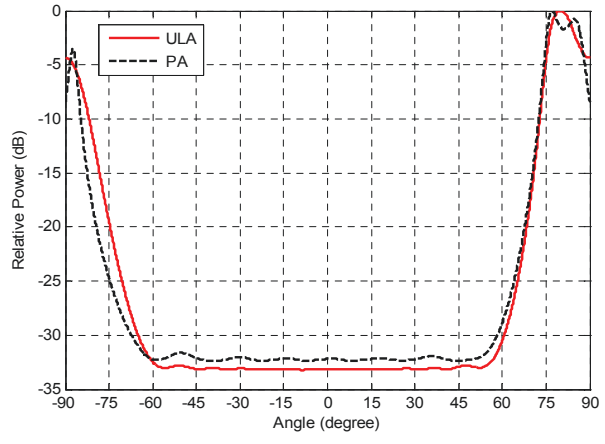

Figure 9 MUSIC spectrum for the ULA and PA geometries at endfire AOAs (76°, 86°), SNR = 10 dB, *K* = 100.

Table 4 Accuracy of MUSIC algorithm in the case of narrowband sources at the border of the spectrum, SNR = 10 dB, *K* = 100

Angles (°)	Success (%)		Average of estimated angles (°)		Variance of estimated angles (°)	
	PA	ULA	PA	ULA	PA	ULA
θ1 = 65	100	100	65.0114	65.0147	0.0110	0.0112
θ2 = 85			84.9744	84.9451	0.1112	0.2465
θ1 = 70	100	98.7	70.0072	70.0391	0.0382	0.0478
θ2 = 87			86.9949	86.9506	0.1976	0.5465
θ1 = 75	93.4	24.4	75.7108	75.9304	0.2364	0.2863
θ2 = 85			84.3999	83.9856	0.4254	0.6843
θ1 = 77	32.9	0.2	78.2324	78.4353	0.2608	0.2510
θ2 = 87			86.1968	83.6095	0.5371	0.2732
θ1 = 78	0.4	0	80.6241	-	0.1386	-
θ2 = 85			83.6816	-	0.4449	-

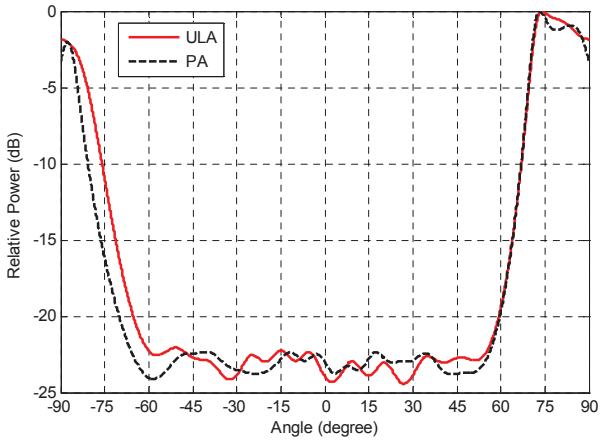

Figure 10 MVDR spectrum for the ULA and PA geometries at endfire AOAs (72°, 86°), SNR = 10 dB, K = 100.

Table 5 Accuracy of MVDR algorithm in the case of narrowband sources at the border of the spectrum, SNR = 10 dB, K = 100

Angles (°)	Success (%)		Average of estimated angles (°)		Variance of estimated angles (°)	
	PA	ULA	PA	ULA	PA	ULA
θ1 = 50	100	99.9	49.9988	49.9992	0.0022	0.0021
θ2 = 87			87.0151	87.0319	0.0767	0.2806
θ1 = 55	100	99.7	54.9965	54.9999	0.0033	0.0026
θ2 = 87			87.0311	87.0608	0.0826	0.2612
θ1 = 60	100	98.4	60.0015	59.9963	0.0050	0.0049
θ2 = 87			86.9832	87.820	0.1049	0.3894
θ1 = 65	100	97.1	65.0621	65.686	0.0128	0.0133
θ2 = 87			86.8584	86.5803	0.1482	0.5512
θ1 = 70	99.5	18.7	70.5040	70.6565	0.0568	0.0801
θ2 = 87			86.4340	85.5583	0.2573	0.3105
θ1 = 75	8	0	76.8038	-	0.0494	-
θ2 = 87			85.6822	-	0.2908	-

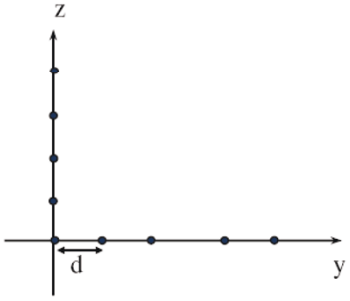

Figure 11 L-shape uniform array.

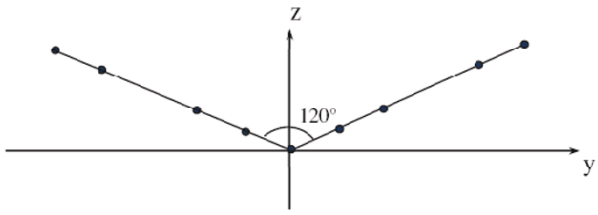

Figure 12 V-shape uniform array.

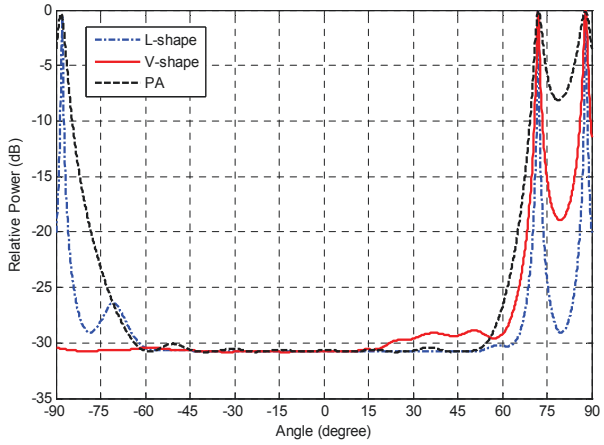

Figure 13 Comparison of MUSIC spectrum in the PA, L-shape and V-shape geometries at endfire AOAs (72°, 88°), SNR = 10 dB, K = 100.

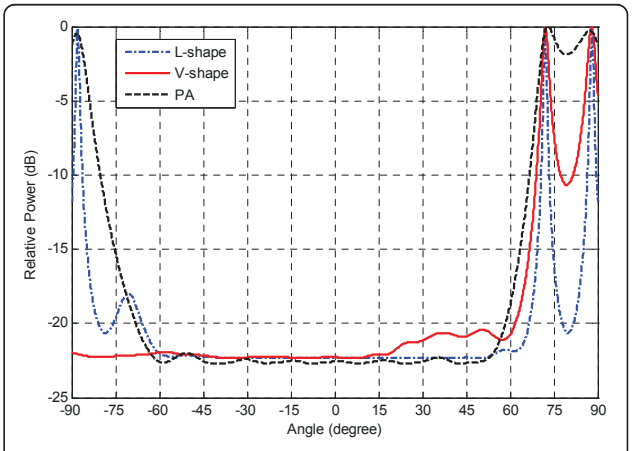

Figure 14 Comparison of MVDR spectrum in the PA, L-shape and V-shape geometries at endfire AOAs (72°, 88°), SNR = 10 dB, K = 100.

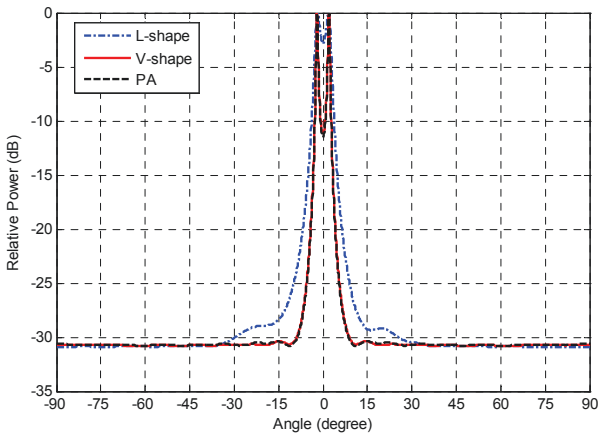

Figure 15 Comparison of MUSIC spectrum in the PA, L-shape and V-shape geometries at boresight directions (-2°, 2°), SNR = 10 dB, *K* = 100.

angle between the V-shape sub-arrays affects the performance of this array. Therefore, the PA is an appropriate and simple geometry for AOA estimation and can modify the performance of the conventional ULA in AOA estimation. This structure may provide the ability of 3-D AOA estimation that can be followed in future works.

Conclusions

The conventional ULA is the most common array geometry for smart antenna systems and array signal processing. Beside great advantages, the ULA does not perform uniform for all angles in the spatial spectrum and cannot detect or resolve close sources located at endfires, accurately. In this article, new ULA-based array geometry is proposed and presented which can remove this drawback by keeping the simplicity in implementation and analysis. Spectral and numerical evaluation is done on the resolution of both ULA and PA geometries via two well-known AOA estimation algorithms, MUSIC as well as MVDR. Simulation results show that the proposed array resolves narrowband signal sources located at close angles to the array endfire accurately, while having a good resolution in other directions. In addition, to improve the performance of the conventional ULA, the PA presents better accuracy and resolution than the L-shape array in boresight directions. The PA also presents near accuracy to the V-shape array with equal element numbers while having less complexity, computational cost and array aperture size.

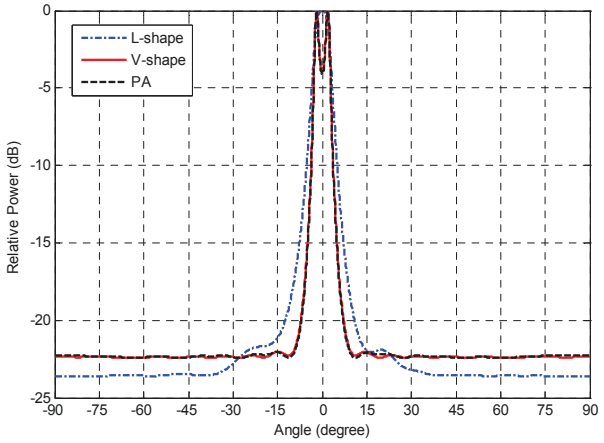

Figure 16 Comparison of MVDR spectrum in the PA, L-shape and V-shape geometries at boresight directions (-2°, 2°), SNR = 10 dB, *K* = 100.

List of abbreviations

AOA: Angle of Arrival; CCI: Co-Channel Interference; DOA: Direction of Arrival; DSA: Displaced Sensor Array; MUSIC: MUltiple SIgnal Classification; MVDR: Minimum Variance Distortionless Response; PA: Proposed Array; RMSE: Root Mean Square Error; SNR: Signal to Noise Ratio; TDOA: Time Difference of Arrival; TOA: Time of Arrival; UCA: Uniform Circular Array; ULA: Uniform Linear Array; URA: Uniform Rectangular Array.

Acknowledgements

This work has been supported by Shahid Rajaee Teacher Training University (SRTTU) under contract number 316 (16.1.1390). We would like to thank anonymous reviewers for their careful reviews of the article. Their comments have certainly improved the quality of this article.

Author details

[1]Digital Communications Signal Processing (DCSP) Research Lab., Faculty of Electrical and Computer Engineering, Shahid Rajaee Teacher Training University (SRTTU), Tehran, Iran [2]Electrical Engineering Department, Tehran South Branch, Islamic Azad University, Tehran, Iran

Competing interests

The authors declare that they have no competing interests.

Received: 15 November 2010 Accepted: 10 August 2011
Published: 10 August 2011

References

1. H Krim, M Viberg, Two decades of array signal processing research. IEEE Signal Process Mag. **July**, 67–94 (1996)
2. F Ji, S Kwong, Robust and computationally efficient signal-dependent method for joint doa and frequency estimation. EURASIP J Adv Signal Process. 1–16 (2008)
3. X Zhang, Y Shi, D Xu, Novel blind joint direction of arrival and polarization estimation for polarization-sensitive uniform circular array. Progress Electromagn Res. **PIER 86**, 19–37 (2008)
4. LC Godara, Application of antenna arrays to mobile communications. part ii: beamforming and direction-of-arrival considerations. Proc IEEE. **85**(8), 1195–1245 (1997). doi:10.1109/5.622504
5. F Gross, *Smart Antennas for Wireless Communications with MATLAB* (McGraw Hill, New York, 2005)
6. M Chryssomallis, Smart Antennas. IEEE Antennas Prop Mag. **42**(3), 129–136 (2000). doi:10.1109/74.848965
7. SW Varade, KD Kulat, Robust algorithms for DOA estimation and adaptive beamforming for smart antenna application. in *Second International Conference on Emerging Trends in Engineering and Technology, ICETET-09*, 1195–1200 (2009)
8. LC Godara, *Handbook of Antennas in Wireless Communications* (CRC Press LLC, New York, 2002)

9. RM Shubair, MA Al-Qutayri, JM Samhan, A setup for the evaluation of MUSIC and LMS algorithms for a smart antenna system. J Commun. **2**(4), 71–77 (2007)
10. U Baysal, RL Moses, On the geometry of isotropic arrays. IEEE Trans Signal Process. **51**(6), 1469–1478 (2003). doi:10.1109/TSP.2003.811227
11. P Ioannides, CA Balanis, Uniform circular arrays for smart antennas. IEEE Antennas Prop Mag. **47**(4), 192–206 (2005)
12. M Lin, L Yang, Blind calibration and DOA estimation with uniform circular arrays in the presence of mutual coupling. IEEE Antennas Wireless Prop Lett. **5**, 315–318 (2006)
13. Y Hua, TK Sarkar, DD Weiner, An L-Shaped array for estimating 2-D directions of wave arrival. IEEE Trans Antenna Prop. **39**(2), 143–146 (1991). doi:10.1109/8.68174
14. N Tayem, HM Kwon, L-Shape 2-dimensional arrival angle estimation with propagator method. IEEE Trans Antenna Prop. **53**(5), 1622–1630 (2005)
15. F Harabi, H Changuel, A Gharsallah, Direction of arrival estimation method using a 2-L shape arrays antenna. Prog Electromagn Res. **PIER 69**, 145–160 (2007)
16. SW Ellingson, Design and evaluation of a novel antenna array for azimuthal angle-of-arrival measurement. IEEE Trans Antenna Prop. **49**(6), 971–979 (2001). doi:10.1109/8.931156
17. WG Diab, HM Elkamchouchi, A deterministic approach for 2D-DOA estimation based on a V-shaped array and a virtual array concept. in *IEEE 19th International Symposium on Personal, Indoor and Mobile Radio Communications*, 1–5 (Sept. 2008)
18. DT Vu, A Renaux, R Boyer, S Marcos, Performance analysis of 2D and 3D antenna arrays for source localization. in *EUSIPCO-2010*, 661–665 (Aug. 2010)
19. T Filik, TE Tuncer, Uniform and nonuniform V-shaped isotropic planar arrays. in *5th IEEE Sensor Array and Multichannel Signal Processing Workshop*, 21–23 (July 2008)
20. L Jin, L Li, H Wang, Investigation of different types of array structures for smart antennas. in *International Conference on Microwave and Millimetre Wave Technology (ICMMT2008)*, April 2008, pp. 1160–1163
21. F Gozasht, GR Dadashzadeh, S Nikmehr, a comprehensive performance study of circular and hexagonal array geometries in the LMS algorithm for smart antenna applications. Prog Electromagn Res. **PIER 68**, 281–296 (2007)
22. RM Shubair, RS Al Nuaimi, Displaced sensor array for improved signal detection under grazing incidence conditions. Prog Electromagn Res. **PIER79**, 427–441 (2008)
23. MA Al-Nuaimi, RM Shubair, KO Al-Midfa, Direction of arrival estimation in wireless mobile communications using minimum variance distortionless response. in *Second International Conference on Innovations in Information Technology (IIT'05)*, 1–5 (Sept. 2005)
24. HC So, Y Wu, Fast algorithm for high resolution frequency estimation of multiple real sinusoids. IEICE Trans Fundam. **E.86-A**(11), 2891–2893 (2003)
25. M Rubsamen, AB Gershman, Direction-of-arrival estimation for nonuniform sensor arrays: from manifold separation to Fourier domain MUSIC methods. IEEE Trans Signal Process. **57**(2), 588–599 (2009)
26. P Stoica, Z Wang, J Li, Robust capon beamforming. IEEE Signal Process Lett. **10**(6), 172–175 (2003). doi:10.1109/LSP.2003.811637
27. T Filik, TE Tuncer, Design and evaluation of V-shaped arrays for 2-D DOA estimation. in *IEEE International Conference on Acoustics, Speech and Signal Processing, 2008, (ICASSP 2008)*, pp. 2477–2480

doi:10.1186/1687-6180-2011-39
Cite this article as: Shirvani-Moghaddam and Akbari: **A novel ULA-based geometry for improving AOA estimation.** *EURASIP Journal on Advances in Signal Processing* 2011 **2011**:39.